

## Use of Twisted Cauchy-Condition Surface to Reconstruct the Last Closed Magnetic Surface in the LHD

ひねりコーシー条件面を用いたLHDの最外殻磁気面逆解析

Gaku Okubo<sup>1)</sup>, Masayuki Akazawa<sup>1)</sup>, Yutaka Matsumoto<sup>1)</sup>, Masafumi Itagaki<sup>1)</sup>,  
Ryosuke Seki<sup>2)</sup>, Yasuhiro Suzuki<sup>2)</sup> and Kiyomasa Watanabe<sup>2)</sup>  
大久保岳<sup>1)</sup>, 赤澤眞之<sup>1)</sup>, 松本裕<sup>1)</sup>, 板垣正文<sup>1)</sup>, 關良輔<sup>2)</sup>, 鈴木康浩<sup>2)</sup>, 渡邊清政<sup>2)</sup>

<sup>1)</sup>Hokkaido University, Kita 13, Nishi 8, Kita-ku, Sapporo 060-8628, Japan

<sup>2)</sup>National Institute for Fusion Science, 322-6 Oroshi-cho, Toki-city, Gifu 509-5292, Japan

<sup>1)</sup>北海道大学, 〒060-8628 札幌市北区北13条西8丁目

<sup>2)</sup>核融合科学研究所, 〒509-5292 岐阜県土岐市下石町322-6

The three-dimensional (3-D) Cauchy condition surface (CCS) method code is now under development to reconstruct the 3-D magnetic field profile in the Large Helical Device (LHD). A new “twisted CCS” has been introduced, whose elliptic cross section rotates with the variation in plasma geometry in the toroidal direction. Independent of the toroidal angle, this CCS can be placed at a certain distance from the last closed magnetic surface (LCMS). With this new CCS, the numerical accuracy in the reconstructed field has been improved. Further, the magnetic field line tracing indicates the LCMS more precisely than with the use of the axisymmetric CCS.

### 1. Introduction

The Cauchy condition surface (CCS), where both the Dirichlet and Neumann conditions are unknown, is placed in a domain that can be supposed to be inside the plasma. In the analysis, no plasma current is assumed outside this CCS. Instead, the CCS plays the same role as the plasma current in causing the field outside the plasma. The choice of suitable shape and size of the CCS is important to assure the accuracy of the reconstructed solution. In the previous work for the Large Helical Device (LHD) [1], the shape of the 3-D CCS was simply assumed to be a torus that has a circular cross section. Instead of this axisymmetric CCS, one here introduces a new idea named “twisted CCS” in order to reduce the numerical error.

### 2. Outline of the 3-D CCS Method [1]

Assuming a vacuum field outside the CCS, three types of boundary integral equations (BIEs), i.e., for magnetic field sensors, flux loops and points along the CCS, are given in terms of 3-D vector potential. They are solved simultaneously in such a way that the vector potential and its derivative on the CCS will be consistent with the sensor signals.

In more detail, the BIEs are discretized, coupled and expressed in the matrix equation form as

$$D\mathbf{p} = \mathbf{g}. \quad (1)$$

Here the solution vector  $\mathbf{p}$  contains the vector potentials and their normal derivatives on the CCS.

In the present work, Eq. (1) is solved using the truncated singular value decomposition technique, where the condition number is kept to be not larger than  $10^5$ . Once all the components in  $\mathbf{p}$  are known,

the magnetic fields for arbitrary points can be calculated.

### 3. Twisted CCS

A larger cross-section of CCS, i.e., a shorter distance between the CCS and a sensor position is better for receiving the sensor signal information. However, the field solution inside the last closed magnetic surface (LCMS) given by the CCS method is, so to speak, turbulence or chaos that exerts a harmful influence on the accuracy of the field profile outside the plasma. From this standpoint, a small size of CCS is a good choice to avoid the numerical instability. Because of this, the cross section of the axisymmetric CCS in the previous work [1] had to be set very small, i.e. a circle having 0.075m radius.

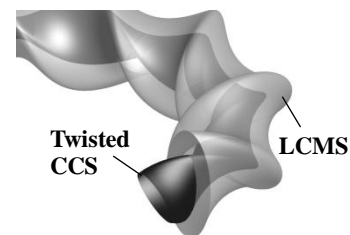


Fig.1. Image of twisted CCS

One here introduces the “twisted CCS” as illustrated in Fig.1, whose elliptic cross section rotates with the variation in vacuum vessel geometry in the toroidal direction. Independent of the toroidal angle, this CCS can be placed at a certain distance from the LCMS. A reduction in the numerical error can then be expected.

The ellipse given by

$$(r - r_0)^2 / a^2 + (z - z_0)^2 / b^2 = 1 \quad (2)$$

rotates 180° clockwise in the poloidal direction when

it proceeds  $36^\circ$  counterclockwise in the toroidal direction following the 10-fold rotational symmetry of the LHD plasma. In this process the variation in the coordinates  $(r, z)$  on the CCS is described as

$$\begin{pmatrix} r - r_0 \\ z - z_0 \end{pmatrix} = \begin{pmatrix} \cos 5\varphi & \sin 5\varphi \\ -\sin 5\varphi & \cos 5\varphi \end{pmatrix} \begin{pmatrix} a \cos(\theta + 5\varphi) \\ b \sin(\theta + 5\varphi) \end{pmatrix}. \quad (3)$$

$(0 \leq \theta \leq 180^\circ, 0 \leq \varphi \leq 36^\circ)$

#### 4. Numerical Examples

One here considers the plasma with a volume-averaged  $\beta$  being  $\langle \beta \rangle = 2.7\%$  in the LHD. The reference field and the sensor signals (126 flux loops and 440 field sensors) for this condition had been calculated beforehand using the HINT2 code [2].

Test calculations were made for (i) the axisymmetric CCS having a 0.075m radius circular cross section, and (ii) the twisted one where the values of  $a$  and  $b$  in Eq. (2) are 0.15m and 0.375m, respectively.

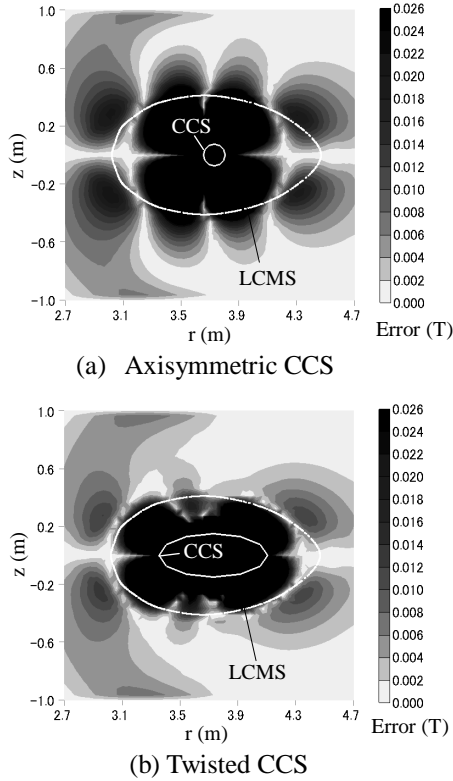


Fig.2. Distribution of absolute error of  $B_r$

Table I. Tendency of the absolute errors of  $B_r$

	Axisymmetric CCS	Twisted CCS
$\varepsilon < 0.01(\text{T})$	43.9%	80.3%
$\varepsilon < 0.005(\text{T})$	24.3%	50.8%
$\varepsilon < 0.001(\text{T})$	5.9%	12.1%
Max. Error	0.042(T)	0.025(T)
Ave. Error	0.013(T)	0.006(T)

Figures 2(a) and 2(b) show the distributions of

absolute error of  $B_r$ , respectively obtained using the axisymmetric CCS and the twisted CCS, both of which are on the  $r$ - $z$  plane at  $\varphi = 18^\circ$  (the horizontal elongated cross section). The absolute errors in the stochastic region are summarized in Table I.

Based on the reconstructed field, magnetic field line tracings were carried out. Figure 3 shows the Poincaré plots on the  $r$ - $z$  plane at  $\varphi = 18^\circ$ . The dashed closed line shows the LCMS for the vacuum field, i.e.,  $\langle \beta \rangle = 0\%$ . This is shifted outward when  $\langle \beta \rangle$  takes the nonzero value  $\langle \beta \rangle = 2.7\%$ . The reference LCMS in this case is the solid closed line. The round symbols show the results of the trace originating at the same starting point as the reference LCMS for  $\langle \beta \rangle = 2.7\%$ , but based on the reconstructed field obtained using the axisymmetric CCS. They do not form a sharp closed surface, however, the round symbols are distributed almost along the reference LCMS for  $\langle \beta \rangle = 2.7\%$ .

The results based on the twisted CCS are shown in Fig. 4. The scatter of the plot points is narrower than in the case of the axisymmetric CCS, i.e., the accuracy in the reconstruction has been significantly improved.

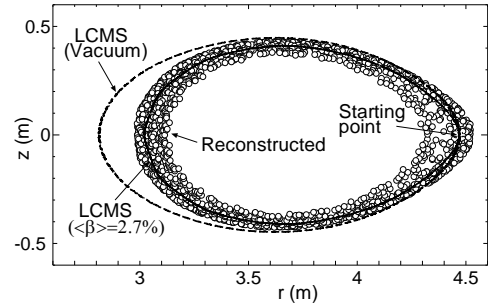


Fig.3. Reconstructed LCMS (Axisymmetric CCS)

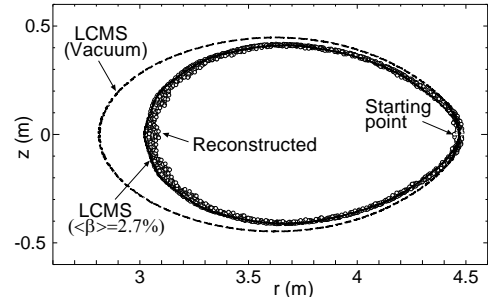


Fig.4. Reconstructed LCMS (Twisted CCS)

#### 5. Conclusion

With the use of the twisted CCS rather than the axisymmetric CCS, the numerical accuracy in the reconstructed field has been improved. Also, the field line tracing indicates the LCMS more precisely.

#### References

- [1] M. Itagaki et al.: *Plasma Phys. Control. Fusion* **53** (2011) 105007.
- [2] Y. Suzuki et al.: *Nucl. Fusion* **46** (2006) L19.